

Predicting prostate movement during early-stage radiotherapy treatment

R. Kojima¹, Y. Tanaka^{2,3}, N. Irie¹, H. Sasaki¹, T. Morishita¹, A. Nakamoto⁴, K. Nishioka⁴, S. Takahashi⁴, Y. Tanabe^{5*}

¹Facility of Health Sciences, Okayama University Medical School, Okayama University, 2-5-1 Shikata, Kita-ku, Okayama, Japan

²Department of Radiological Technology, Graduate School of Health Sciences, Okayama University, 2-5-1, Shikata, Kita, Okayama, Japan

³Office of Project Management, Division of Moonshot Research and Development Program, 1-6-1 Nagata-cho, Chiyoda-ku, Tokyo, Japan

⁴Department of Radiology, Tokuyama Central Hospital, 1-1 Kodacho, Shunan, Yamaguchi, Japan

⁵Faculty of Medicine, Graduate School of Health Sciences, Okayama University, 2-5-1 Shikata, Kita-ku, Okayama, Japan

ABSTRACT

► Original article

***Corresponding author:**

Yoshinori Tanabe, Ph.D.,

E-mail:

tanabey@okayama-u.ac.jp

Received: September 2024

Final revised: March 2025

Accepted: April 2025

Int. J. Radiat. Res., October 2025;
23(4): 973-977

DOI: 10.61186/ijrr.23.4.20

Keywords: Prostate cancer, two-plane analysis, prostate movement, setup errors, adaptive radiation therapy.

Background: Predicting the direction and amount of movement of the patient-specific prostate at an early stage of treatment is important for estimating systematic errors and avoiding large dose differences between planning and actual treatment. This study aimed to evaluate a two-plane analysis of prostate movement for multiple-image matching and examine the accuracy of predicting the amount of prostate movement for inter- and intra-fraction setup errors at the early stage of treatment.

Materials and Methods: Sixty-five patients who underwent prostate intensity-modulated rotating radiotherapy with fiducial markers were examined for setup errors in bone matching and inter- and intra-marker matching. The two-plane setup errors in the anterior-posterior (AP), left-right (LR), and superior-inferior (SI) directions were analyzed. Correlation analysis was performed by calculating the relationship between the total average setup error and each average setup error (2–5 fractions), increasing from the first to the sixth fraction. **Results:** The inter- and intra-fraction setup errors between the AP and SI directions of prostate movement were moderately correlated ($r: 0.63$, $r = 0.58$, respectively). The average setup error of >4 fractions was strongly correlated ($r > 0.7$), and the standard deviation of the >3 fraction setup errors was moderately correlated ($r > 0.4$) with total and early setup errors. **Conclusions:** Prostate movement during radiotherapy was linear in the AP-SI direction. The evaluation of early fraction setup errors may be used to predict prostate movement in individual patients during the treatment period.

INTRODUCTION

Prostate cancer has a high occurrence frequency and mortality rate in men; however, the progression of symptoms is relatively slow⁽¹⁾. Prostate cancer is often treated with surgery and radiation therapy, and intensity-modulated rotational radiation therapy (IMRT) enables a steep dose-gradient distribution owing to an increase in the dose concentration on the target^(2, 3).

In prostate volumetric modulated arc therapy (VMAT), the target prostate is close to organs at risk (OAR), such as the rectum, bladder, and small bowel, and universality of positional coordinates between organs is required during the treatment period. However, the prostate and surrounding OAR change the relationship of positional coordinates owing to peristalsis and tension, rectum gas, and bladder filling, limiting dose reduction to organs at risk⁽⁴⁾.

Therefore, prostate VMAT is important for observing individual patients and predicting changes in the relationship between positional coordinates during the treatment period to avoid overdosing for OAR or underdosing for the target^(5, 6).

In previous studies, we predicted prostate movement in advance using diagnostic computerized tomography (CT) and multiple planning CTs to reduce the deviation between the planned treatment and actual treatment dose; however, prediction using multiple planning CTs increases the exposure dose^(7, 8).

Adaptive radiation therapy is used to address changes in positional coordinates of the target and OAR using cone beam CT (CBCT), and target movement and OAR need attention owing to the short irradiation duration⁽⁹⁾. Robust radiotherapy is effective for the short-term movement of organs, and a robust plan requires the accurate prediction of

patient-specific organ movement (9, 10). Predicting complete organs before treatment planning is difficult because of the extension of the start of treatment and the increase in radiation exposure due to multiple planned CT scans (7). In image-guided radiotherapy, matching images are often obtained using CBCT, which can be used to evaluate daily organ movements and trends in patient-organ movements (7, 10, 11). Considering the advantages and disadvantages of adaptive and robust radiotherapy, predicting the trend of patient organ movements for the early fraction is effective (12). In addition, early identification of an individual's prostate movement can lead to re-planning, avoiding large differences between planned and actual doses (13-15).

To date, no study has investigated the relationship between the two-plane prostate movement and prediction methods for patient-specific prostate movement management at the early fraction stage using CBCT. Therefore, this study aimed to evaluate two-plane prostate movement for robust planning and accuracy in predicting prostate movement at the early fraction stage of treatment for offline adaptive and robust radiotherapy. In the early stages, the tendency of a patient's prostate to move helps improve the quality and safety of patient-specific radiotherapy.

MATERIALS AND METHODS

Patients and materials

This study included 65 patients (median age, 72 [57-82] years) who underwent prostate VMAT with fiducial markers implanted in the prostate. This study was approved by the Ethics Committee of the Institutional Review Board (IRB) of Tokuyama Central Hospital and was conducted in accordance with the ethical guidelines of the Declaration of Helsinki (IRB K456-20230201).

Patients with prostate cancer were scanned using a CT Aquilion LB scanner (Toshiba Medical Systems, Tokyo, Japan), and CT images were acquired using the radiotherapy treatment-planning system Eclipse version 11 (Varian Medical Systems, Palo Alto, CA, USA). The implanted fiducial markers were treated with a Novalis STX linear accelerator (Varian Medical Systems, Palo Alto, CA, USA) attached to an ExacTrac X-ray system (BrainLAB AG, Feldkirchen, Germany). Knee braces and foot pillows were used as immobilizers. All patients underwent rectal emptying and bladder filling before the planned CT and treatment. All the patients received a total radiation dose of 78 Gy in 39 fractions.

Calculation of setup error of three types of image matching

Digitally reconstructed radiographs (DRR) of radiotherapy-planning CT scans were created using a

radiotherapy planning system based on image matching. The setup error of the three types of image matching was calculated using bone and inter- and intra-fraction fiducial marker matching. The setup error of bone matching was different between the pelvic bone and skin markers using the DRR and ExacTrac X-ray systems. The setup error of inter-fractional fiducial marker matching was calculated by image matching before and after treatment using the DRR and ExacTrac X-ray systems. Each setup error was calculated as the anterior-posterior (AP), superior-inferior (SI), left-right (LR) directions, and 3D distance. The 3D distance was calculated using the equation (1):

$$3D\ distance = \sqrt{(AP_{SE})^2 + (LR_{SE})^2 + (SI_{SE})^2} \quad (1)$$

Where; AP_{SE} , LR_{SE} , and SI_{SE} were setup errors in each direction.

Evaluation of two plane setup error of three types of image matching

The median, standard deviation (SD), and 95th percentile of setup errors of the three types of image matching were calculated for AP, LR, SI direction, and 3D distances using the statistical software SPSS (IBM, Chicago, IL, USA). Next, the correlation coefficients (r) of the two-plane setup errors in the AP, LR, and SI directions were analyzed using SPSS.

Prediction of systematic and random setup error of patient-specific prostate movement at the early fraction stage

To evaluate the prediction accuracy for systematic and random setup errors of patient-specific prostate movement during the treatment period, the average and SD of the setup error for the entire duration of treatment were compared with that of the early fraction stage. The average and SD of the setup error at the early fraction stage were calculated for five different treatment periods (1-2, 1-3, 1-4, 1-5, and 1-6 fraction) for AP, LR, SI direction, and 3D distance. The correlation coefficient (r) of the average and SD of the setup error between the entire duration of treatment and five different treatment periods was analyzed using statistical software SPSS.

Statistical analysis

The correlation coefficient (r) of the setup error was analyzed by linear approximation using the statistical software SPSS.

RESULTS

Table 1 presents the median, minimum, and maximum values of patients' average setup errors in bone and inter- and intra-marker matching. The median values (SD) of the 3D distances for setup errors in bone and marker matching during

treatment were 5.2 (1.8) mm, 3.0 (0.7) mm, and 1.1 (0.85) mm. (Table 1). The average treatment time for 65 patients was 87.2 sec (range: 71.5–15.0 sec). The 95th percentile of bone matching and inter- and intra-fraction setup errors were 9.1, 3.4, and 1.4 mm in the AP direction; 5.1, 1.3, and 0.9 mm in the LR direction; and 5.2, 5.5, and 1.9 mm in the SI direction, respectively. The 95th percentile of intra-fraction marker matching against inter-fraction marker matching was decreased by approximately half or less in the AP and SI directions, and slightly decreased in the LR direction.

The inter- and intra-marker setup errors were moderately correlated in the AP-SI direction, and no correlation was observed in the other two plane directions (figure 1).

The correlation coefficients tended to be higher according to increasing fraction average number for the average and SD of the setup error for the entire duration of treatment (table 2, figures 2 and 3). The average setup errors >4 fractions at the early fraction stage had a strong correlation ($r > 0.7$), and the SD of setup errors >3 fractions had a moderate correlation ($r > 0.4$) (table 2).

Table 1. Setup error for each image matching.

Set up error (mm)	Bone matching median (range)	Inter-marker matching median (range)	Intra-marker matching median (range)
Average	AP -2.8 (-10.0–7.1)	0.93 (-4.1–5.3)	-0.1 (-1.0–3.3)
	LR 0.1 (-5.6–7.6)	0.4 (-1.5–1.2)	0.0 (-0.9–1.8)
	SI 1.1 (-3.1–5.8)	0.4 (-7.1–7.0)	0.0 (-1.0–4.7)
	3D 5.2 (2.9–10.8)	3.0 (1.2–8.9)	1.1 (0.5–6.3)
SD	AP 2.3 (1.3–3.9)	1.6 (0.6–3.5)	0.8 (0.4–1.9)
	LR 1.5 (0.7–3.6)	0.5 (0.3–1.2)	0.4 (0.1–1.4)
	SI 1.3 (0.9–4.5)	1.4 (0.7–3.6)	0.7 (0.3–2.5)
	3D 1.8 (1.1–3.4)	1.3 (0.5–4.2)	0.9 (0.2–2.2)

SD: standard deviation, AP: anterior-posterior, LR: left-right, SI: superior-inferior.

Table 2. Relationship of average intra-fraction setup error between the entire duration of treatment and five different treatment periods at the early fraction stage.

Correlation: r		Fraction 1-2 ave.	Fraction 1-3 ave.	Fraction 1-4 ave.	Fraction 1-5 ave.	Fraction 1-6 ave.
Average	Inter	AP 0.74	0.80	0.79	0.82	0.84
		LR 0.65	0.75	0.75	0.75	0.75
	Intra	SI 0.79	0.86	0.87	0.89	0.90
		3D 0.59	0.72	0.69	0.79	0.83
SD	Inter	AP 0.66	0.67	0.72	0.73	0.79
		LR 0.77	0.86	0.90	0.90	0.91
	Intra	SI 0.79	0.77	0.79	0.79	0.80
		3D 0.85	0.88	0.90	0.92	0.94

SD: standard deviation, AP: anterior-posterior, LR: left-right, SI: superior-inferior, ave.: average.

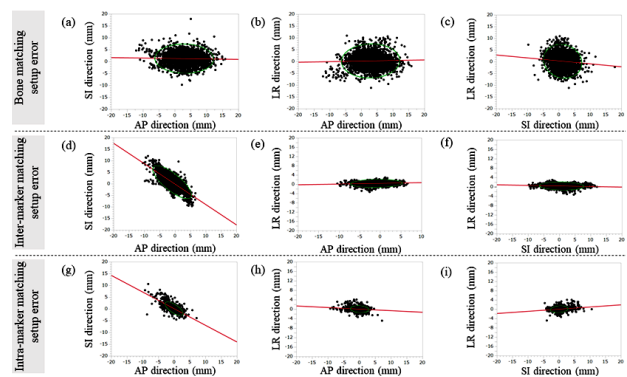


Figure 1. Relationship of two plane setup error for bone matching and inter- and intra-fraction marker matching. Bone matching: (a) SI-AP direction ($r = 0.00$), (b) LR-AP direction ($r = 0.0$), (c) LR-SI direction; Inter-fraction marker matching: (d) SI-AP direction ($r = 0.61$), (e) LR-AP direction ($r = 0.01$), (f) LR-SI direction ($r = 0.01$), Intra-fraction marker matching: (g) SI-AP direction ($r = 0.51$), (h) LR-AP direction ($r = 0.02$), (i) LR-SI direction ($r = 0.03$). Ellipses in the figure indicate the 95% confidence intervals. SI: superior-inferior, AP: anterior-posterior, LR: left-right. This figure was referred the Figure 4 of reference15 Sasaki *et al.*, 2024.

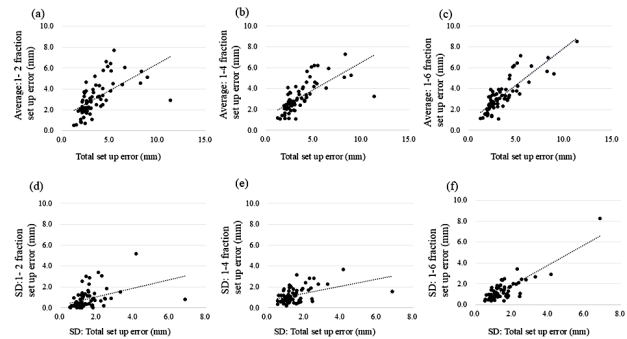


Figure 2. Relationship of average inter-fraction setup error of 3D distance between the entire duration of treatment and 3 kinds of treatment period at the early fraction stage for 3D distance. Average: (a) first and second fraction, (b) first to fourth fraction, (c) first to sixth fraction, Standard deviation (SD): (d) first and second fraction, (e) first to fourth fraction, (f) first to sixth fraction.

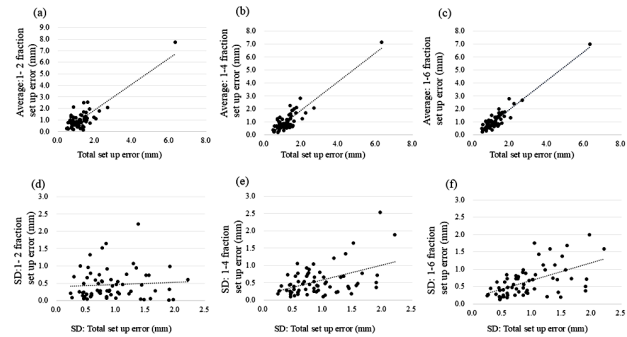


Figure 3. Relationship of average intra-fraction setup error of 3D distance between the entire duration of treatment and 3 kinds of treatment period at the early fraction stage. Average: (a) first and second fraction, (b) first to fourth fraction, (c) first to sixth fraction, Standard deviation: (d) first and second fraction, (e) first to fourth fraction, (f) first to sixth fraction.

DISCUSSION

This study evaluated the two-plane setup error for bone and inter- and intra-fraction marker matching. In addition, the trend in patient-specific prostate movements was evaluated using image-matching results in the early fractional stage.

The stepwise correction of the geometric position in image-guided radiotherapy was evaluated from bone matching to marker matching (15). The 95th percentile of the SI direction in the inter-fraction setup error showed a larger movement compared with that of bone matching. The median of intra-fraction setup error was close to zero in the LR and SI directions, considering that image matching was able to match the geometric center of the prostate movement. The 95th percentile of intra-fraction marker matching setup error was decreased by approximately half the value in the AP and SI directions compared with that of inter-fraction marker matching setup error, and the prostate movement was <2 mm in the 95th percentile of average 87 s during treatment time. However, the prostate movement occurred even after as little as 87 s of treatment time. Therefore, we considered that the control of prostate movement is not complete after image matching, and paying attention to the dose impact of intra-fraction movement during an average treatment time of 87 s is necessary (16, 17).

In a two-plane analysis of setup errors, the bone matching setup error was the 95% confidence interval value close to concentric circles for the SD of the SI-LR directions. The SD of bone matching may affect changes in body weight and mood, such as relaxation or tension, during the treatment period (13, 14). Furthermore, prostate movement in the AP-SI direction was moderately correlated in inter- and intra-fraction. This is believed to be due to the restriction of movement in the AP-SI direction by the adjacent bladder and rectum around the prostate (15, 17). We considered that the directionality of prostate movement in the AP-SI is anatomically located around the adjacent bladder and rectum and can be observed via the contraction of pelvic floor muscles and peristalsis of the intestinal movement (8, 18). In addition, understanding a patient's specific directionality of prostate movement will help in margin setting before planning and robust radiotherapy at the time of treatment (19).

In predicting early radiotherapy for patient-specific systematic and random errors, the average setup errors of both the inter- and intra-fraction were highly accurate, in accordance with the average number of fractions increasing with a strong correlation in >4 fractions. In our previous research, the prediction of a patient's prostate movement was a problem of exposure dose and limited time by multi-plan CT before planning, which could be predicted and re-planned by evaluating systematic setup errors

using ions without scanning additional images. Moreover, the prostate movement of individual patients was evaluated in advance by multiple planned CT scans in the early radiotherapy treatment period (16, 20).

In the prediction of setup at early radiotherapy, the SD of the inter- and intra-fraction were moderately correlated, with >4 fractions in all directions, and the SD of SI and 3D distance had a high correlation of >5 fractions in the inter-fraction setup errors. The correlation coefficient of the SD was lower than that of the average setup error. Therefore, we considered that the average setup error is easy to predict owing to the systematic error of a patient's anatomy and condition in the volume of the bladder and rectum, and the SD is difficult to predict owing to random errors, such as tension of the bladder filling limit and movement of intestinal gas. The relationship SD between the entire duration of treatment and the early treatment period had a moderate correlation of >2 fractions in the LR direction. Hence, the reason for the high accuracy prediction in the LR direction may be attributed to its lower susceptibility to random errors, such as tension, and may also be attributed to anatomical information, such as fat mass and pelvis size (18).

A limitation of this study is that the direction of prostate movement and anatomical information could not be compared and evaluated, and the factors of the two-plane movement direction could not be objectively evaluated. Movement in the LR direction may depend on patient-specific information, and movement prediction may be more accurate by adding anatomical text information.

CONCLUSION

The two-plane prostate movements for the inter- and intra-fraction showed moderately correlated directional movements in the AP-SI direction. In the inter- and intra-fraction, the average setup error could be predicted with a strong correlation using setup data of >4 fractions, and the SD of the setup error at the early fraction stage could be predicted to be moderately correlated. This method predicts the tendency of a patient's prostate movement and helps improve the quality and safety of patient-specific radiotherapy by avoiding systematic errors.

Acknowledgment: This work was supported by JSPS KAKENHI (grant number: JP23K07063).

Conflict of interest: None.

Funding: This work was supported by JSPS KAKENHI (grant number: JP23K07063).

Ethical consideration: This study was approved by the Ethics Committee of the Institutional Review Board (IRB) of Tokuyama Central Hospital and was conducted in accordance with the ethical guidelines

of the Declaration of Helsinki (IRB K456-20230201). **Author contributions:** Y.T., R.K.: Conceptualization, methodology, formal analysis, writing - original draft. N.I., H.S., Y.T.: Conceptualization, data curation. T.M., A.N., K.N.: Conceptualization, resources, data curation, formal analysis. Y.T., S.T.: Formal analysis, writing - review & editing.

Possible AI usage for manuscript preparation: None.

REFERENCES

1. Rawla P (2019) Epidemiology of prostate cancer. *World J Oncol*, **10** (2): 63-89. doi: 10.14740/wjon1191.
2. Martin JM, Frantzis J, Eade T, Chung P (2010) Clinician's guide to prostate IMRT plan assessment and optimization. *J Med Imaging Radiat Oncol*, **54**(6): 569-75. doi:10.1111/j.1754-9485.2010.02217.x.
3. Bauman G, Rumble RB, Chen J, Loblaw A, Warde P (2012) Members of the IMRT Indications Expert Panel. Intensity-modulated radiotherapy in the treatment of prostate cancer. *Clin Oncol*, **24** (7): 461-73. doi: 10.1016/j.clon.2012.05.002.
4. Colvill E, Poulsen PR, Booth JT, O'Brien RT, Ng JA, Keall PJ (2014) DMLC tracking and gating can improve dose coverage for prostate VMAT. *Med Phys*, **41**(9): 091705. doi: 10.1118/1.4892605.
5. Venkatesan K, Raphael CJ, Varghese KM, Gopu P, Sivakumar S, Boban M, et al. (2020). Volume and dosimetric analysis of rectum and bladder for prostate carcinoma patients by using kilo voltage cone beam computed tomography (CBCT). *Int J Radiat Res*, **18**(3): 557-569. doi: 10.18869/acadpub.ijrr.18.3.557.
6. Mahdavi SR, Gharehbagh EJ, Mofid, B, Jafari A H, Nikoofar AR (2017). Accuracy of the dose delivery in prostate cancer patients using an electronic portal imaging device (EPID). *Int J Radiat Res*, **15**(1): 39. doi: 10.18869/acadpub.ijrr.15.1.39.
7. Tanabe Y and Ishida T (2019) Optimizing multiple acquisition planning CT for prostate cancer IMRT. *Biomed Phys Eng Express*, **5** (3): 035011. doi: 10.1088/2057-1976/ab0dc7.
8. Tanabe Y, Ishida T, Eto H, Sera T, Emoto Y (2019) Evaluation of the correlation between prostatic displacement and rectal deformation using the Dice similarity coefficient of the rectum. *Med Dosim*, **44**(4): e39-43. doi: 10.1016/j.meddos.2018.12.005.
9. Pathmanathan AU, van As NJ, Kerkmeijer LGW, Christodouleas J, Lawton CAF, Vesprini D, et al. (2018) Magnetic resonance imaging-guided adaptive radiation therapy: a "game changer" for prostate treatment? *Int J Radiat Oncol Biol Phys*, **100**(2): 361-73. doi: 10.1016/j.ijrobp.2017.10.020.
10. Boubaker MB, Haboussi M, Ganghoffer JF, Aletti P (2009) Finite element simulation of interactions between pelvic organs: predictive model of the prostate motion in the context of radiotherapy. *J Biomech*, **42**(12): 1862-8. doi:10.1016/j.jbiomech.2009.05.022.
11. Budiharto T, Slagmolen P, Haustermans K, Maes F, Junius S, Verstraete J, et al. (2011) Intrafractional prostate motion during online image guided intensity-modulated radiotherapy for prostate cancer. *Radiat Oncol*, **98**(2): 181-6. https://doi.org/10.1016/j.radonc.2010.12.019.
12. Kiriyma T, Fukui A, Ishikawa H, Doi M, Nishimoto Y, Cyosei K, Kishimoto K, Tanabe Y (2025). Efficacy of hydrogel spacer compared with intensity-modulated radiotherapy for 3-dimensional conformal radiotherapy for prostate cancer. *Med Dosim*, in press. doi:10.1016/j.meddos.2025.01.005.
13. Tanabe Y and Eto H (2022) Evaluation of patient-specific motion management for radiotherapy planning computed tomography using a statistical method. *Med Dosim*, **47**(2): e13-8. doi: 10.1016/j.meddos.2021.12.002.
14. Tanabe Y, Ishida T, Eto H, Sera T, Emoto Y, Shimokawa M (2021) Patient-specific radiotherapy quality assurance for estimating actual treatment dose. *Med Dosim*, **46**(1): e5-e10. doi:10.1016/j.meddos.2020.08.003.
15. Sasaki H, Morishita T, Irie N, Kojima R, Kiriyma T, Nakamoto A, Nishioka K, Takahashi S, Tanabe, Y. (2024). Evaluation of the trend of set-up errors during the treatment period using set-up margin in prostate radiotherapy. *Med Dosim*, **49**(4): 291-297. doi: 10.1016/j.meddos.2024.02.004.
16. Brand VJ, Milder MT, Christianen M E, Hoogeman MS, Incrocci L (2022) Seminal vesicle inter-and intra-fraction motion during radiotherapy for prostate cancer: A review. *Radiat Oncol*, **169**: 15-24. doi: 10.1016/j.radonc.2022.02.002.
17. Feng SQ, Brouwer CL, Korevaar EW, Vapiwala N, Kang-Hsin Wang KK, Deville Jr C, et al. (2023) Dose evaluation of inter- and intra-fraction prostate motion in extremely hypofractionated intensity-modulated proton therapy for prostate cancer. *Phys Imaging Radiat Oncol*, **27**: 100474. doi: 10.1016/j.phro.2023.100474.
18. Sihono DSK, Ehmann M, Heitmann S, von Swietochowski S, Grimm M, Boda-Heggemann J, et al. (2018) Determination of intrafraction prostate motion during external beam radiation therapy with a transperineal 4-dimensional ultrasound real-time tracking system. *Int J Radiat Oncol Biol Phys*, **101**(1): 136-43. doi: 10.1016/j.ijrobp.2018.01.040.
19. Yagihashi T, Inoue K, Nagata H, Yamanaka M, Yamano A, Suzuki S, et al. (2023) Effectiveness of robust optimization against geometric uncertainties in TomoHelical planning for prostate cancer. *J Appl Clin Med Phys*, **24**(4): e13881. doi: 10.1002/acm2.13881.
20. Tanabe Y, Ishida T, Eto H, Sera T, Emoto Y (2020) Optimizing planning CT using past CT images for prostate cancer volumetric modulated arc therapy. *Med Dosim*, **45**(3): 213-8. doi: 10.1016/j.meddos.2019.12.008.

